Journal of Mechanical Science and Technology (KSME Int. J.), Vol. 19, No. 8, pp. 1649~1661, 2005 **1649**

Heat Transfer of an Evaporating Liquid on a Horizontal Plate

Sang Woo Joo, Min Soo Park*, Min Suk Kim
School of Mechanical Engineering, Yeungnam University, Gyongsan, 712-749, Korea

We consider a horizontal static liquid layer on a planar solid boundary. The layer is evaporating when the plate is heated. Vapor recoil and thermo-capillary are discussed along with the effect of mass loss and vapor convection due to evaporating liquid and non-equilibrium thermodynamic effects. These coupled systems of equations are reduced to a single evolution equation for the local thickness of the liquid layer by using a long-wave asymptotics. The partial differential equation is solved numerically.

Key Words: Thermo-Capillary, Evaporating Liquid, Long-Wave Approximation, Evolution Equation

Nomenclature

C : Capillary number
D : Distance between solid surface and water pipe
D_ρ : Ratio of the liquid density and vapor density
D_ν : Ratio of the liquid kinematic viscosity and vapor kinematic viscosity
d_b : Mean film thickness
d_b : Dimensionless solid plate thickness
E : Evaporation number
G : Non-dimensional measure of gravity g
H : Curvature
h : Liquid depth
h_r : Heat transfer coefficient of vapor
$\bar{I}$: Identity tensor
J : Mass flux
K : The degree of non-equilibrium at the evaporating interface
L : Latent heat
$\vec{n}$: Normal vector at liquid surface
M : Maragoni number
p : Pressure
Pr : Prandtl number
R_s : Ratio for the thermal conductive coefficient of solid and vapor
S : Non-dimensional surface tension
$\bar{T}$: Stress tensor
T : Temperature
T_D : Temperature at $z=D$
T_{sat} : Saturated temperature
$\vec{t}$: Tangential vector at liquid surface
$\vec{v}$: Velocity vector for
t : Time
κ : Thermal diffusivity
σ_0 : Surface tension at the reference temperature
Γ : Ratio of thermal diffusivity
θ_r : Rupture time
Φ : Non-dimensional temperature
$\bar{\tau}$: The ratio of deformation tensors
ρ : Density
μ : Dynamic viscosity
ν : Kinematic viscosity

Subscripts

b : Bottom of solid plate
s : Ratio of solid property and liquid property
v : Ratio of vapor property and liquid property

Superscripts

v : Vapor phase
s : Solid phase
I : Liquid-vapor interface

* Corresponding Author,
E-mail: mspark@yu.ac.kr
TEL: +82-53-810-3239; **FAX**: +82-53-813-3703
School of Mechanical Engineering, Yeungnam University, Gyongsan, 712-749, Korea. (Manuscript **Received** November 19, 2003; **Revised** June 21, 2005)

1. Introduction

A liquid layer lies on a planar solid plate in Fig. 1. There is a mode of instability present when the layer is thin which is driven, even in a static layer, and results in the rupture of the layer. Such a film possesses a difference in chemical potential with respect to a large phase of the same materials resulting in a corresponding change in all intensive thermodynamic properties.

The problem of finding the film thickness which becomes unstable owing to Van der Waals forces was considered by Vrij (1966). He used a static stability analysis to calculate a marginally stable thickness at which small disturbances start to grow. A dynamics linear stability theory for an isothermal film on a horizontal plate (Rukenstein, 1974) based on the Navier-Stokes equations modified with an extra body force due to Van der Waals attractions. It shows that an initial disturbance periodic along the bounding plane has a critical wavelength much larger than the mean depth of the layer. Gummerman (1975) examined the linear stability of radically bounded thinning free films for which the base state is a time-dependent drainage flow computed by lubrication theory. Williams (1982) posed a nonlinear stability based on the long-wave nature of the response. They derived a partial differential equation describing the evolution of the interfaced shape subject to surface tension and viscous force. Davis (1983) discussed the generalization of the result to a non-volatile film on a heated plate, accounting for thermo-capillary and gravity wave effects.

This study considers the previous work conditions as thin liquid states on the heated solid plate and as the transition of phase is motivated due to evaporating, not due to boiling. As the time becomes large, the liquid comes to be evaporating, and the evaporating liquid motivates convection in the vapor. In this study, we are going to consider three-coupled phases for heat transfer with the governing equations and their boundary conditions, obtain the equations for surface displacement by the long-wave asymptotics, and apply for the approximation method and numerical method to understand liquid film behavior.

2. Mathematical Model

2.1 Theoretical Analysis

The basic concept of the evaporating liquid on a horizontal plate is established in Fig. 1, where it can be assumed that a liquid layer is thin enough that gravity effects are negligible, but thick enough that a continuum theory of the liquid is applicable. The liquid layer exists over the solid plate that has dimensionless thickness d_b, and a vapor layer contacts over the liquid. It can be defined that coordination is $x-z$ direc-

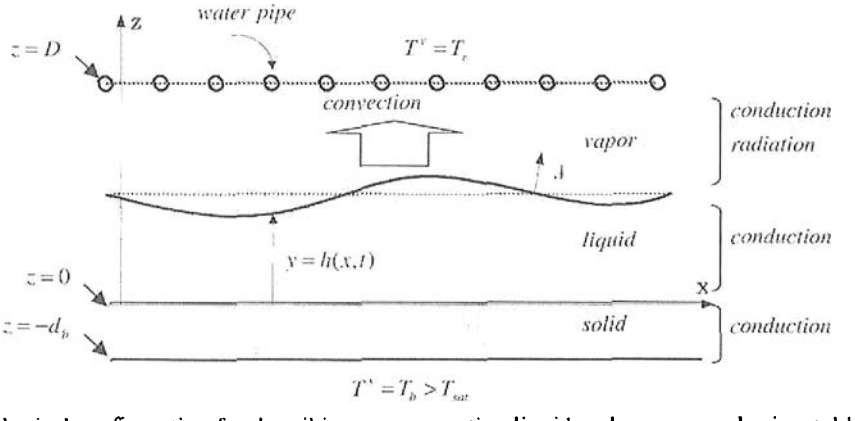

Fig. 1 The physical configuration for describing an evaporating liquid and vapor on a horizontal heated solid plate

tion, the corresponding velocity is $\vec{v}=\vec{v}(u, w)$, mass flux is $J=(x, t)$, and temperature is $T=T(x, t)$. At $z=D$ we assume the vapor temperature might be maintained to the constant temperature due to water pipe, and at $z=-d_b$ the source temperature at the bottom of the solid plate might be maintained to a constant temperature that is bigger than T_{sat}. The interface between liquid and vapor can be located in $z=h(x, t)$ and the evaporation occurs in a direction normal to the interface. The other physical configurations are introduced in Fig. 1. In solid plate the conduction can be applied. In liquid layer the conduction can be applied, but the convection can be ignored due to the film-like thickness of liquid. In the vapor layer the conduction, the convection and the radiation are considered. The unit vector $\vec{n}$ and $\vec{t}$ are the outward normal and tangential direction as, respectively,

$$\vec{n}=(-h_x, 1)(1+h_x^2)^{-(1/2)}$$
$$\vec{t}=(1, h_x)(1+h_x^2)^{-(1/2)} \quad (1)$$

In Fig. 1, the normal vector is up to vapor direction for moving boundary problem for which the three phases interact with the variation of displacement and time. Thus, it can be called Multi-Phase, Free-Boundary Problem.

We need the three governing equations in the liquid and in the vapor and the energy equation in the solid as

$$u_x+w_z=0,\ u_x^v+w_z^v=0 \quad (2)$$

$$\rho(\vec{v}_t+\vec{v}\cdot\nabla\vec{v})=-\nabla p+\mu\nabla^2\vec{v}$$
$$\rho^v(\vec{v}_t^v+\vec{v}^v\cdot\nabla\vec{v}^v)=-\nabla p+\mu\nabla^2\vec{v} \quad (3)$$

$$T_t=\kappa\nabla^2T,\ T_t^v=\kappa^v\nabla^2T^v,\ T_t^s=\kappa^s\nabla^2T^s \quad (4)$$

We also need the boundary conditions such as the temperature boundary condition at $z=-d_b$, the temperature boundary condition and energy balance at $z=0$, the continuous temperature condition at $z=D$, and the continuous temperature condition, jump mass balance, jump energy balance, normal-stress boundary condition, and share-stress boundary condition at $z=h(x, t)$ referred to Delhaye (1974). They are, respectively,

At $z=-d_b$

$$T^s=T_b \quad (5)$$

At $z=0$

$$T^s=T,\ k^sT_z^s=kT_z \quad (6)$$

At $z=D$

$$T^v=T_D \quad (7)$$

At $z=h(x, t)$

$$T=T^v \quad (8)$$

$$J=\rho(\vec{v}-\vec{v}^I)\cdot n=\rho(\vec{v}^v-\vec{v}^I)\cdot n \quad (9)$$

$$J\left[L+\frac{1}{2}\{(\vec{v}^v-\vec{v}_I)\cdot\vec{n}\}^2-\frac{1}{2}\{(\vec{v}-\vec{v}^I)\cdot\vec{n}\}^2\right]$$
$$+k\nabla T\cdot\vec{n}-k^v\nabla T^v\cdot\vec{n}+h_r(T^v|_{z=h}-T^v|_{z=D}) \quad (10)$$
$$+2\mu(\vec{\tau}\cdot\vec{n})\cdot(\vec{v}-\vec{v}^I)-2\mu(\vec{\tau}\cdot\vec{n})\cdot(\vec{v}^v-\vec{v}^I)=0$$

$$J(\vec{v}-\vec{v}^v)\cdot\vec{n}-(\bar{\bar{T}}-\bar{\bar{T}}^v)\cdot\vec{n}\cdot\vec{n}=2\Delta\cdot\vec{n}\sigma(T) \quad (11)$$

$$J(\vec{v}-\vec{v}^v)\cdot\vec{t}-(\bar{\bar{T}}-\bar{\bar{T}}^v)\cdot\vec{n}\cdot\vec{t}=-\nabla\sigma\cdot\vec{t} \quad (12)$$

We assume no slip condition at the interface between the two viscous fluids as $(\vec{v}-\vec{v}^v)\cdot\vec{t}=0$.

The linearized constitutive equation derived from Kinetic theory of Palmer (1976) is shown as

$$J=\left(\frac{\alpha\rho^vL}{T_{sat}^{2/3}}\right)\left(\frac{M_w}{2\pi R_g}\right)^{1/2}(T^I-T_{sat}) \quad (13)$$

It relates the mass flux (J) to the local surface temperature (T^I), where M_w is the molecular weight, R_g is the universal gas constant, and α is the accommodation coefficient. We should consider another constitutive equation for the effect of density variation that is related to the convection in vapor. This is because we do not ignore the convective effect ignored by Burelbach (1988) in corresponding to the evaporating liquid. It can be shown as

$$w^v=\frac{\rho-\rho^v}{\rho}v^I \quad (14)$$

2.2 Dimensionless equations

To make the governing equations and boundary conditions dimensionless, the scale of length

should be considered as the relation to thickness of vapor and liquid with the length (D). So, we can scale the length, the time, the velocity and the pressure with, respectively, D, D^2/ν, ν/D, $\rho\nu^2/D$, where ν is kinematic viscosity of the liquid. The temperature can be scaled as $\Delta T = T_b - T_{sat}$. The mass flux can be scaled as its initial value for a linear temperature profile across an initially flat film $\kappa\Delta T/DL$. Therefore, the dimensionless variables of velocity, temperature, and pressure for each phase can be obtained as

$$\vec{v}^{v\prime}=\frac{D}{\nu}\vec{v}^{v},\ \vec{v}'=\frac{D}{\nu}\vec{v} \tag{15}$$

$$p^{v\prime}=\frac{D^2}{\rho\nu^2}p^{v},\ p'\frac{D^2}{\rho\nu^2}p \tag{16}$$

$$T^{v\prime}=\frac{T^{v}-T_{sat}}{\Delta T},\ T'=\frac{T-T_{sat}}{\Delta T}$$
$$T^{s}=\frac{T^{s}-T_{sat}}{\Delta T} \tag{17}$$

With the scaled variables, Eqs. (2)~(4) are changed as, respectively, (the dimensionless variables are marked with Apostrophe. From now they should be marked without Apostrophe for convenience.)

$$u_x^v+w_z^v=0 u_x+w_z=0 \tag{18}$$

$$D_\rho(\vec{v}_t^v+\vec{v}^v\cdot\nabla\vec{v}\nu)=-\nabla p^v+\nabla^2\vec{v}^v$$
$$\vec{v}_t+\vec{v}\cdot\nabla\vec{v}=-\nabla p+\nabla^2\vec{v} \tag{19}$$

$$\mathrm{Pr}(T_t^v+\vec{v}^v\cdot\nabla T^v)=\Gamma_v T_{zz}^v$$
$$\mathrm{Pr}\,T_t=T_{zz},\ \mathrm{Pr}\,T_t^s=\Gamma_s T_{zz}^s \tag{20}$$

The boundary condition at $z=-d_b$ is

$$T^s=1 \tag{21}$$

At $z=0$, the no-slip condition, the no-penetration condition, the continuum for temperature and thermal flux can be obtained as, respectively,

$$u=0,\ w=0,\ T^s=T,\ R_s T_z^s=T_z \tag{22}$$

At $z=1$ the temporal temperature condition can be obtained as

$$T^v=\Theta \tag{23}$$

At $z=h(x,t)$ we need the constitutive equations related to mass balance condition, energy equilibrium, normal stress equilibrium, shear stress equilibrium, viscous condition, continuous temperature condition, and evaporation condition. These interfacial conditions were introduced by Delhaye (1974), and Burelbach (1988) rearranged these conditions step by step. The continuous temperature condition is

$$T=T^v \tag{24}$$

The mass balance condition is

$$EJ=(\vec{v}=\vec{v}^I)\cdot n=D_\rho(\vec{v}^v-\vec{v}^I)\cdot n \tag{25}$$

The energy balance condition is

$$J+\frac{E^2}{2L}(D_\rho-1)J^3+\Delta T\cdot\vec{n}$$
$$-R_v\nabla T^v\cdot\vec{n}+H(T^v|_{z=h}-T^v|_{z=D})$$
$$+\frac{2}{L'}(\tilde{\tau}\cdot\tilde{n})\cdot(\vec{v}-\vec{v}^I)J$$
$$-\frac{2D_v}{L'}(\tilde{\tau}\cdot\vec{n})\cdot(\vec{v}^v-\vec{v}^I)J=0 \tag{26}$$

In Eq. (25) the first term means the needed energy for the evaporation, the second term means the transformation of momentum energy of evaporated molecular, the third and forth term means the pure thermal flux due to conduction, the fifth term is for thermal flux due to the radiation, and the sixth and seventh term are for dispersion due to viscosity. The normal stress is

$$(1-D\rho)E^2J^2+p-2\tilde{T}\cdot\vec{n}\cdot\vec{n}-p^v$$
$$-2\tilde{T}^v\cdot\vec{n}\cdot\vec{n}=S[1-CT]\nabla\cdot\vec{n} \tag{27}$$

We assume that the vapor and the liquid are incompressible Newtonian fluids. The stress tensor ($\tilde{T}$) is written as $\tilde{T}=p\tilde{I}+2\mu\tilde{\tau}$. Surface tension is represented by a linear equation of state, $\sigma=\sigma_0-\gamma(T^I-T_{sat})$. For common liquids $\gamma=-d\sigma/dT$ are positive. The shear stress condition at is

$$\tilde{T}\cdot\vec{n}\cdot\vec{t}-\tilde{T}^v\cdot\vec{n}\cdot\vec{t}=-\frac{M}{\mathrm{Pr}}\nabla T\cdot\vec{t} \tag{28}$$

Eqs. (13) and (14) can be changed as, respectively

$$KJ=T,\ w^v=(1-D_\rho)\vec{v}^I \tag{29}$$

The evaporation equation related to the evaporation and condensation at interface with nonequilibrium is introduced by Scharge (1953)

showing the evaporation model Eq. (28) expressing the linearized equations related to the amount of evaporation and dimensionless temperature in case that there is less non-equilibrium rate, where the parameter K measures the degree of non-equilibrium at the evaporating interface. If $K=0$ it corresponds to the quasi-equilibrium limit, where the interfacial temperature is constant and equal to the saturation value ($T=0$). $K^{-1}=0$ means the non-volatile case in which the evaporative mass flux is zero. The equilibrium state is predictable for $J=0$ in the Eq. (28) when $T=0$. If $T>0$, $J>0$ (the evaporation state). If $T<0$, $J<0$ (the condensation state). Some dimensionless parameters produced in Appendix A.

In component form, the scaled governing system is as following

The continuity equations are

$$u_x+w_z=0 \tag{30}$$

$$u_x^v+w_z^v=0 \tag{31}$$

The momentum equations are

$$u_t+uu_x+wu_z=-p_x+u_{xx}+u_{zz} \tag{32}$$

$$w_t+uw_x+ww_z=-p_z+w_{xx}+w_{zz} \tag{33}$$

$$D_\rho(u_t^v+u^vu_x^v+w^vu_z^v)=-p_x^v+u_{xx}^v+u_{zz}^v \tag{34}$$

$$D_\rho(w_t^v+u^vw_x^v+w^vw_z^v)=-p_z^v+w_{xx}^v+w_{zz}^v \tag{35}$$

The energy equations are

$$\mathrm{Pr}(T_t=uT_x+wT_z)=T_{xx}+T_{zz} \tag{36}$$

$$\mathrm{Pr}(T_t^v+u^vT_x^v+w^vT_z^v)=\Gamma_v(T_{xx}+T_{zz}) \tag{37}$$

$$\mathrm{Pr}\,T_t^s=\Gamma_s(T_{xx}^s+T_{zz}^s) \tag{38}$$

The boundary conditions Eqs. (21) ~ (24) are not changed. Eqs. (25) ~ (28) are changed, respectively, as

$$EJ=(-h_t-uh_x+w)(1+h_x^2)^{-1/2} \tag{39}$$

$$\begin{aligned}&J+\frac{E^2}{2L}(D_\rho-1)J^3\\&+(1+h_x^2)^{-1/2}[T_xh_x-T_z-R^v(T_z^v-T_x^v-T_x^vh_x)]\\&+H[(T^v|_{z=h}-T^v|_{z=0})]\\&+\frac{2J}{L(1+h_x^2)^{1/2}}[h_x(u_z+w_x)-(h_x^2-1)u_x\\&-D_vh_x(u_z^v+w_x^v)-(h_x^2-1)u_x^v]=0\end{aligned} \tag{40}$$

$$\begin{aligned}&(1-D_\rho)E^2J^2+p-2(1+h_x^2)^{-1}[(h_x^2-1)u_x-h_x(u_z+w_x)]\\&-p_v+2D_\rho(1+h_x^2)^{-1}[(h_x^2-1)u_x^v-h_x(u_z^v+w_x^v)]\\&=S[1-CT]h_{xx}(1+h_x^2)^{-3/2}\end{aligned} \tag{41}$$

$$\begin{aligned}&(1-h_x^2)(u_z+w_x)-4h_xu_x\\&-D_\rho[(1-h_x^2)(u_z^v+w_x^v)-4h_x^vu_x^v]\\&=-\frac{M}{\mathrm{Pr}}(T_x+T_{zhx})(1+h_x^2)^{1/2}\end{aligned} \tag{42}$$

Eq. (29) are changed as, respectively,

$$KJ=T,\ w^v=(1-D_\rho)h_t \tag{43}$$

3. Solutions of Approximation Method

3.1 Basic state solutions

The state of the evaporation depends on time because liquid and vapor is on the state of evaporation, and we can consider the assumption that the velocity of evaporation exists only z-direction and there is no velocity in liquid and flat status of the liquid surface. We note that basic state quantities by 'overbar' and rescales time on the evaporative time scale to retain the effect of mass loss in the kinematic condition as

$$R_v=E\bar{R}_v,\ D_\rho=E^{-2}\bar{D}_\rho,\ t'=Et,\ z'=z \tag{44}$$

The dependent variables are expended in powers of E:

$$\bar{T}^v=E^{-1}(T_0^v+ET_1^v+E^2T_2^v+\cdots) \tag{45}$$

$$\bar{T}=T_1+ET_1+E^2T_2+\cdots \tag{46}$$

$$\bar{T}^s=T_0^s+ET_1^s+E^2T_2^s+\cdots \tag{47}$$

$$\bar{J}=J_0+EJ_1+E^2J_2+\cdots \tag{48}$$

$$\bar{w}^v=E^{-1}(w_0^v+Ew_1^v+E^2w_2^v+\cdots) \tag{49}$$

$$\bar{p}=E^{-1}(p_0+Ep_1+E^2p_2+\cdots) \tag{50}$$

$$\bar{p}^v=p_0^v+Ep_1^v+E^2p_2^v+\cdots \tag{51}$$

The momentum equations of the liquid and vapor can be obtained as, respectively,

$$p_{0z'}=0,\ D_\rho p_{0z'}^v=0 \tag{52}$$

The energy equations of the liquid, vapor and solid can be obtained as, respectively,

$$T_{0z'z'}=0,\ \mathrm{Pr}w_0^v T_{0z'}^v = T_{0z'z'}^v\ \ T_{0z'}^s=0 \quad (53)$$

The boundary conditions can be obtained as

$$T_0^s=1 \text{ at } z'=-d_b \quad (54)$$

$$T_0^s=T_0,\ R_s T_{0z'}^s = T_{0z'} \text{ at } z=0 \quad (55)$$

$$T_0^v=\Theta \text{ at } z'=1 \quad (56)$$

The continuous temperature condition, mass balance, energy balance and two constitutive equations at $z'=\bar{h}(t')$ can be shown as, respectively,

$$\begin{gathered} T_0^v=0,\ J_0=-\bar{h}_{t'} \\ J_0+T_{0z'}-\bar{R}_v T_0^v+H(T_0-\Theta)=0 \\ KJ_0=T_0,\ w_0^v=-\bar{D}_\rho h_{t'} \end{gathered} \quad (57)$$

To obtain the effect of the conduction and convection in vapor phase, the second order of the perturbed equation is needed. For the second order, the Navier-Stokes equation for the liquid and the vapor can be obtained as, respectively,

$$p_{1z'}=0,\ D_\rho p_{1z'}^v=0 \quad (58)$$

The energy equation for the liquid, vapor and solid can be obtained as, respectively,

$$T_{1z'z'}=0,\ T_{1z'z'}^v-\frac{\mathrm{Pr}}{\Gamma_v}w_0^v T_{1z'}^v=0,\ T_{1z'z'}^s=0 \quad (59)$$

The boundary conditions can be obtained as

$$T_1^s=1 \text{ at } z'=-d_b \quad (60)$$

$$T_1^s=T_1,\ R_s T_{1z'}^s = T_{1z'} \text{ at } z'=0 \quad (61)$$

$$T_1^v=\Theta \text{ at } z'=1 \quad (62)$$

The continuous temperature condition, mass balance, energy balance and two constitutive equations at $z'=\bar{h}(t')$ can be shown as, respectively,

$$\begin{gathered} T_0=T_{1z'},\ J_1=0 \\ J_1+T_{1z'}-\bar{R}_v T_{1z'}^v+H(T_1-\Theta)=0 \\ KJ_1=T_1,\ w_1^v=0 \end{gathered} \quad (63)$$

Second order equations for more exact solution can be obtained from the same process introduced above. With the initial conditions, $t'=0$, $\bar{h}=0.9$, and the boundary conditions, the solution for basic state can be obtained as

$$\bar{h}(t)=\left[\left(0.9+K+\frac{d_b}{R_s}\right)^2-2Et\right]^{1/2}-K-\frac{d_b}{R_s} \quad (64)$$

$$\bar{J}(t)=\left[\left(0.9+K+\frac{d_b}{R_s}\right)^2-2Et\right]^{1/2} \quad (65)$$

$$\bar{T}^s(z)=\frac{\Pi_1 z-R_s\Pi_2}{R_s\Pi_2+d_b\Pi_1}+\frac{\Pi e^{\Pi h}\Pi_3(z+1)}{R_s(e^{\Pi}-e^{\Pi h})(R_s\Pi_2+d_b\Pi_1)} \quad (66)$$

$$\bar{T}(z)=R_s\frac{\Pi_1 z-\Pi_2}{R_s\Pi_2+d_b\Pi_1}+E\frac{R_v\Pi e^{\Pi h}\Pi_3(R_s z+1)}{R_s(e^{\Pi}-e^{\Pi h})(R_s\Pi_2+d_b\Pi_1)} \quad (67)$$

$$T_v(z)=\frac{(e^{\Pi}-e^{\Pi h})\Pi_3}{(e^{\Pi}-e^{\Pi h})(R_s\Pi_2+d_b\Pi_1)} \quad (68)$$

where Π, Π_1, Π_2, Π_3 are in Appendix A. In the present work, the physical properties of liquid, WATER, are used in the simulation. Detailed data are listed in Appendix A.

3.2 Solutions of surface behavior by evolution equation

To obtain the evolution equation of representing surface behavior, the ratio of the initial average liquid thickness to frequency of the liquid wave is assumed to be very small, it is noted ε, and hence the assumption is allowed to apply for long-wave approximation which was worked by Oron (1997). There are rescaled-independent variables rearranged as

$$\xi=\varepsilon x,\ \zeta=z,\ \tau\varepsilon t \quad (69)$$

All independent variables are transformed for ε order except liquid thickness as Eqs. (86)-(95). Rearranging the variables to be functions of ξ, ς and τ, they are, for the vapor,

$$u^v=\varepsilon^{-2}(u_0^v+\varepsilon u_1^v+\varepsilon^2 u_2^v+\cdots) \quad (70)$$

$$w^v=\varepsilon^{-1}(w_0^v+\varepsilon w_1^v+\varepsilon^2 w_2^v+\cdots) \quad (71)$$

$$p^v=p_0^v+\varepsilon p_1^v+\varepsilon^2 p_2^v+\cdots \quad (72)$$

$$T^v=\varepsilon^{-1}(T_0^v+\varepsilon T_1^v+\varepsilon^2 T_2^v+\cdots) \quad (73)$$

for the liquid,

$$u=\varepsilon(u_0+\varepsilon u_1+\varepsilon^2 u_2+\cdots) \quad (74)$$

$$w=\varepsilon(w_0+\varepsilon w_1+\varepsilon^2 w_2+\cdots) \quad (75)$$

$$p=\varepsilon^{-1}(p_0+\varepsilon p_1+\varepsilon^2 p_2+\cdots) \quad (76)$$

$$T=T_0+\varepsilon T_1+\varepsilon^2 T_2+\cdots \quad (77)$$

and, for the solid,

$$T^s = T_0^s + \varepsilon T_1^s + \varepsilon^2 T_2^s + \cdots \tag{78}$$

Mass flux can be expressed as

$$J = J_0 + \varepsilon J_1 + \varepsilon^2 J_2 + \cdots \tag{79}$$

We also represent the following dimensionless parameters for including all the remaining physical effect in this model as $\mathrm{Pr} = \varepsilon\overline{\mathrm{Pr}}$, $E = \varepsilon\bar{E}$, $M = \varepsilon\bar{M}$, $D_\rho = \varepsilon^{-2}\bar{D}_\rho$, $S = \varepsilon^{-2}\bar{S}$, $D_\mu = \varepsilon^{-2}\bar{D}_\mu$ where, Over Bar indicates O(1). For the leading-order equations, all governing equations and boundary conditions are arranged by $O(\varepsilon)$ using with Eq. (69). Continuity equations for liquid and vapor can be obtained as, respectively,

$$w_{0\zeta} = 0,\ w_{0\zeta}^v = 0 \tag{80}$$

Navier-stokes equation for liquid can be expressed as

$$p_{0\xi} = 0,\ p_{0\zeta} = 0 \tag{81}$$

Energy equations for liquid, vapor and solid can be expressed as, respectively,

$$T_{0\zeta\zeta} = 0,\ \frac{\overline{\mathrm{Pr}}}{\Gamma_v} w_0^v T_{0\zeta}^v = T_{0\zeta\zeta}^v,\ T_{0\zeta\zeta}^s \tag{82}$$

Boundary conditions can be obtained as

$$T_0^s = 1 \text{ at } \zeta = -d_B \tag{83}$$

$$w_0 = 0,\ T_0^s = T_0,\ R_s T_{0\zeta}^s = T_{0\zeta} \text{ at } \zeta = 0 \tag{84}$$

$$T^v = 0 \text{ at } \zeta = 1 \tag{85}$$

Boundary conditions for continuous temperature condition, mass balance, energy balance, normal stress balance and shear stress balance at $\zeta = h(\xi, \tau)$ can be obtained as, respectively,

$$\begin{gathered} T_0^v = 0,\ \bar{E} J_0 = w_0 - h_\tau,\ J_0 + T_{0\zeta} = \bar{R}_v T_{0\xi}^v = 0 \\ p_0 = 0,\ u_{0\zeta} = \frac{\bar{M}}{\overline{\mathrm{Pr}}} (T_{0\xi} + T_{0\zeta} h_\xi) \end{gathered} \tag{86}$$

The two constitutive equations at $\zeta = h(\xi, \tau)$ can be expressed as, respectively,

$$K J_0 = T_0,\ w_0^v = -\bar{D}_\rho h_\tau \tag{87}$$

The results of the first order equations can be obtained as

$$h(\tau) = \left[\left(0.9 + K + \frac{d_b}{R_s}\right) - 2E\tau\right]^{\frac{1}{2}} - K - \frac{d_b}{R_s} \tag{88}$$

$$w_0^v = \frac{(D_\rho - 1)\bar{E} R_s}{R_s(K+h) + d_b} \tag{89}$$

$$J_0 = \frac{R_s}{R_s(K+h) + d_b} \tag{90}$$

$$T_0^s = \frac{R_s(K+h) - \zeta}{R_s(K+h) + d_b} \tag{91}$$

$$T_0 = \frac{R_s(K+h-\zeta)}{R_s(K+h) + d_b} \tag{92}$$

$$T_0^v = 0 \tag{93}$$

Second order equations for more exact solution can be obtained from the same process introduced above. Thus the solution for long-wave approximation can be obtained as

$$\begin{aligned} T^s(z) &= \frac{R_s K - \Pi_1(R_s h + z)}{R_s \Pi_2 + d_b \Pi_1} \\ &+ \frac{\Pi_2 e^{\Pi h}\{\Pi_1(R_s h + d_b)\Theta + R_s K(\Theta - 1)\}(z+1)}{R_s(e^{\Pi} - e^{\Pi h})\{(\Pi_1(R_s h + d_b)) + R_s K\}} \end{aligned} \tag{94}$$

$$\begin{aligned} T(z) &= \frac{R_s K - R_s \Pi_1(h+z)}{R_s \Pi_2 + d_s \Pi_1} \\ &+ \frac{E R_v \Pi e^{\Pi h}\{\Pi_1(d_b + R_s h)\Theta + R_s K(\Theta - 1)\}(R_s z + 1)}{R_s(e^{\Pi} - e^{\Pi h})\{\Pi_1(R_s h + d_s) + R_s K\}} \end{aligned} \tag{95}$$

$$T_v(z) = \frac{\{\Pi_1(R_s h\Theta + d_b\Theta) + K R_s\Theta\}(e^{\Pi z} - e^{\Pi h}) + K R_s(e^{\Pi} - e^{\Pi z})}{(e^{\Pi} - e^{\Pi h})\{\Pi_1(R_s h + d_b) + R_s K\}} \tag{96}$$

The pressure, evaporation rate and evaporation velocities for liquid can be obtained as (cf. Appendix A)

$$p = G(h - z) + \frac{R_B D_\rho E^2}{(R_s(K+h) + d_b)^2} - S h_{xxx} \tag{97}$$

$$J = \frac{R_s}{\Pi_4} + \frac{R_v \Pi e^{\Pi h}(h R_s + d_b)(\Pi_4 \Theta - R_s K)}{(e^{\Pi h} - e^{\Pi})\Pi_4} \tag{98}$$

$$u = \left(S h_{xxx} + \frac{\Pi_5 h_x}{\Pi_4^3} - G h_x\right)\left(hz - \frac{z^2}{2}\right) - \frac{M}{\mathrm{Pr}}\left(\frac{R_s}{\Pi_4}\right)_x z \tag{99}$$

$$\begin{aligned} w &= \left(S h_{xxx} + \frac{\Pi_4 \Pi_5 h_x - 3 R_s \Pi_5 h_x^2}{\Pi_4^4} - G h_{xx}\right)\left(\frac{h z^2}{2} - \frac{z^3}{6}\right) \\ &+ \frac{1}{2} h_x z^2 \left(S h_{xxx} + \frac{\Pi_5 h_x}{\Pi_4^3} - G h_x\right) - \frac{M}{2\,\mathrm{Pr}}\left(\frac{R_s}{\Pi_4}\right)_{xx} z^2 \end{aligned} \tag{100}$$

The evolution equation expressing surface behavior can be obtained as

$$h_t+EJ+\left[\left(\frac{S}{3}\right)h^3h_{xxx}+\left(\frac{R_s^2KM}{2\mathrm{Pr}\prod_4^2}\right)h^2h_x +\left(\frac{2D_\rho R_s^3E^2}{3\prod_4^3}+\frac{G}{3}\right)h^3h_x\right]_x=0 \quad (101)$$

We need Finite Differential Method to solve the forth order nonlinear partial equation. It is solved numerically in conservative form as part of an initial-value problem for spatially periodic solutions on the fixed interval $0<x<2\pi/k_M$. Crank-Nicholson in time and central differences in space are employed. The difference equations are solved by Newton-Raphson method until error$<10^{-8}$. The solution of temperature distribution is proceeded after solving Eq. (101). The initial state for these equations is

$$h(x,\,0)=0.5-0.1\cos(k_Mx),\ k_M=2^{-1/2} \quad (102)$$

with the disturbance having the frequency $2\pi/k_M$.

4. Results and Discussions

4.1 Discussion for basic state

Since the liquid on the heated plate is evaporating, the basic state is time-dependent. The basic state is assumed to be static with a flat evaporating interface. Thus, there is no dependence of the lateral coordination, and the basic-state velocity of the field is zero. When $\Theta=1$ at $z=1$ the water pipe temperature is equal to the solid temperature at bottom and when $\Theta=-1$ at $z=1$ the water pipe temperature is as low as the difference between the solid temperature at bottom and the saturated temperature. When it is quasi-equilibrium evaporation ($K=0$) the temperature difference across the film is constant, so that the heat flux and the evaporation rate are expected to be larger where the film is thinner, and when it is non-equilibrium evaporation ($K\neq0$) the interface temperature depends on the fluxes.

Figure 2 shows the rate of the height reduction in quasi-equilibrium evaporation is faster than that of the height reduction in non-equilibrium case as the time becomes large. It means that K makes the evaporation velocity disturbed (cf. Bankoff, 1971). Fig. 3 shows the variation of mass flux in basic-state when $\Theta=1$ at $z=1$. The rate of increasing mass loss from the liquid in the quasi-equilibrium evaporation is larger than that of increasing mass loss from the liquid in the non-equilibrium case. It can be resulted that the film is so thin that the heat from the solid plate is likely to accelerate evaporating velocity without increasing the temperature of the liquid-vapor

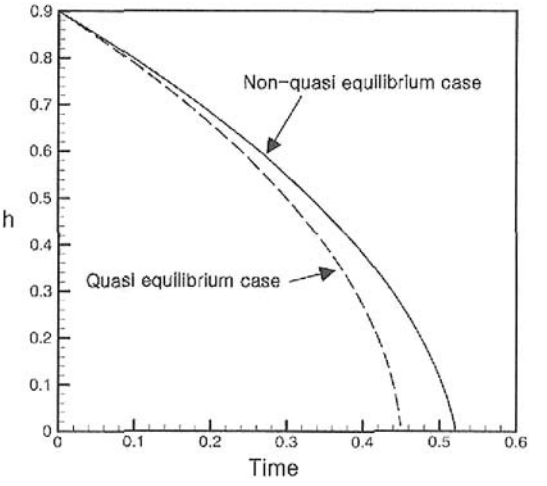

Fig. 2 The variation of liquid thickness of basic state when $\Theta=1$ at $z=1$. Dimensionless thickness of liquid is initially 0.9

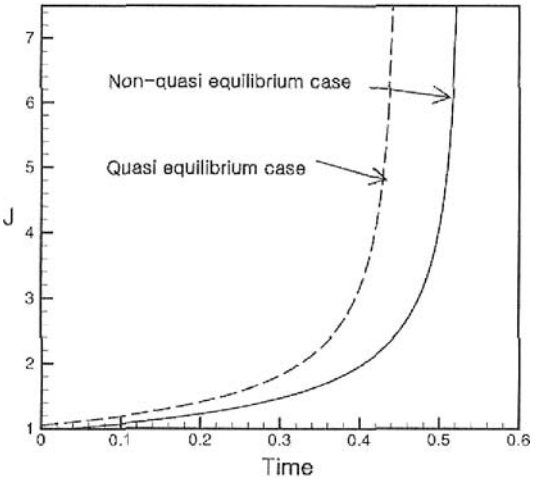

Fig. 3 Variation of mass flux of basic state when $\Theta=1$ at $z=1$

interface comparing with the non-equilibrium case.

Figs. 4 and 5 show the variation of temperature distribution of basic-state with an instant film thickness (h=0.001, 0.05, 0.2, 0.4, 0.6, 0.8, and 0.9) respectively when $\Theta=1$ and $\Theta=-1$ at $z=1$, where the vertex of the lines is the interface of the phases. As the time becomes large, the temperature through solid and liquid comes to increase, and the height of the liquid comes to decrease. The temperature at the interfaces comes to be lower than the previous state because the evaporative rate is increasing and the space between the liquid-vapor interface and the water pipe becomes wider that it takes more time for the temperature to lose the energy to the surrounding. As Figs. 4 and 5 describe, two interfaces eventually meet together in Fig. 6 showing the variation of the temperature of two interfaces.

4.2 Quasi-equilibrium evaporation ($K=0$)

In the case of the quasi-equilibrium evaporation ($K=0$), the surface temperature becomes constant because of the disturbance in the film evaporation phenomenon, and the mass flux and the evaporative effect are stronger in the thinner

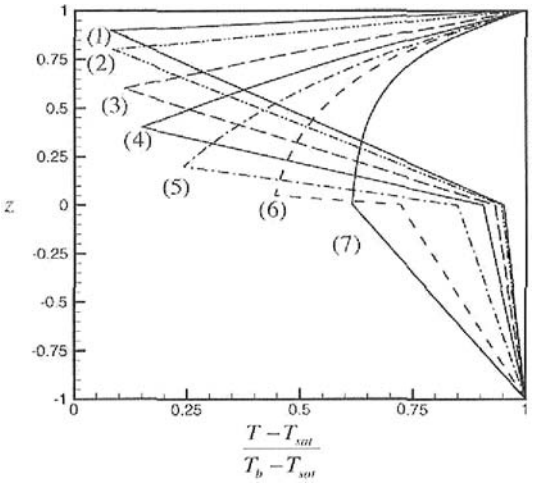

Fig. 4 Variation of temperature distribution of basic state when $\Theta=1$ at $z=1$. Line (1), (2), (3), (4), (5), (6) and (7) state when instant film thickness (h) is 0.9 (initial value), 0.8, 0.6, 0.4, 0.2, 0.05 and 0.001 respectively, where the bottom of solid plate at $z=-1$, the top of solid plate is at $z=0$, and the water pipe is at $z=1$

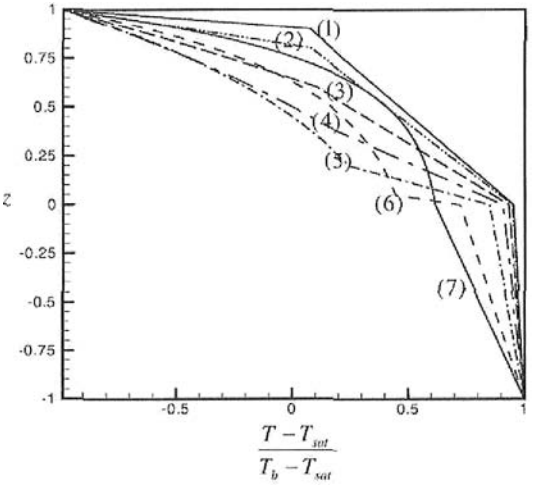

Fig. 5 The variation of temperature distribution of basic state when $\Theta=-1$ at $z=1$. Line (1), (2), (3), (4), (5), (6) and (7) state when instant film thickness (h) is 0.9 (initial value), 0.8, 0.6, 0.4, 0.2, 0.05 and 0.001 respectively, where the bottom of solid plate at $z=-1$, the top of solid plate is at $z=0$, and the water pipe is at $z=1$

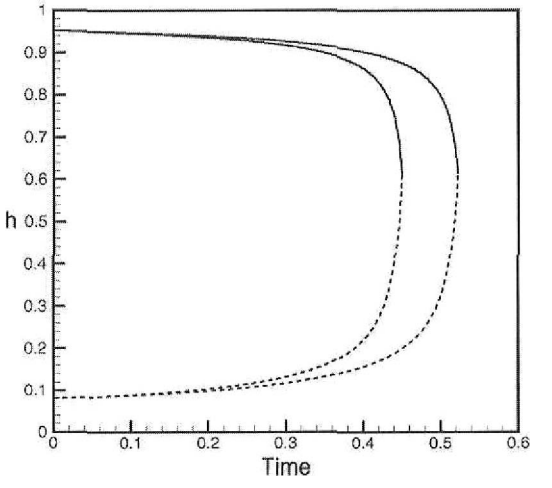

Fig. 6 The variation of temperature at the interface when $\Theta=1$ at $z=1$. Solid line and dot line are solid-liquid interface and vapor-liquid interface, respectively. Outer line and inner lines are non-quasi equilibrium case and non-quasi equilibrium case, respectively. They finally meet together

film region.

To obtain surface behavior in the quasi-equilibrium we set $K=0$ in Eq. (101) and the result is

$$h_t+EJ+\left[\left(\frac{S}{3}\right)h^3h_{xxx}+\left(\frac{2D_\rho R_s^3E^2}{3(R_sh+d_b)^3}+\frac{G}{3}\right)e^3h_x\right]_x=0 \tag{103}$$

The parametercan S be removed from Eq. (103) by rescaling with

$$X=(1/S)^{1/2}x,\ \theta=(1/S)t \tag{104}$$

Eq. (103) can be obtained as the canonical form ;

$$h_\theta+\Im J+\frac{1}{3}(h^3h_{xxx})_x+\frac{1}{3}\left[\left(\frac{2R_s\Re}{R_sh+d_b}+G\right)h^3e_x\right]_x=0 \tag{105}$$

$\Im$ is an effect of mass loss ($\Im=ES$) and $\Re$ is an effect of vapor recoil ($\Re=D_\rho E^2$). Vapor recoil effect meets at 'Trough' than 'Crest' in the film wave and results in being unstable. Let $\Re=1$ for $\Im=0$, 0.3, 0.6 and 1, respectively, figure the wave behavior. Fig. 7 shows that the mass loss is expected to increase due to the effect of the vapor coil, moreover it is shown that the larger the value of $\Im$ is the shorter the rupture time (θ_r) is. Let $\Im=1$ for $\Re=0$, 0.3 and 1, respectively, figure the film wave profile. It is clear that the larger the value of the vapor coil is, the shorter the rupture time. However the effect to the reduction of the rupture time (θ_r) becomes less than the previous condition in Fig. 8.

4.3 Non-equilibrium evaporation ($K\neq0$)

We now allow $K\neq0$ from Eq. (101) for non-equilibrium evaporation. In this case the temperature of the interface depends on the flux. We can rescale it with Eq. (104) and obtain non-equilibrium evaporation equation form as

$$h_\theta+\Im J+\left[\frac{1}{3}h^3h_{xxx}\right]_x+\left[\left(\frac{R_s^2K}{2\Pi_4^2}\right)\Omega h^2h_x+\left(\frac{2R_s^3}{3\Pi_4^3}\Re+\frac{G}{3}\right)h^3h_x\right]_x=0 \tag{106}$$

The term proportional to $\Omega\ (=M\ \mathrm{Pr}^{-1})$ represented the thermocapillary effect can be obtained. The profiles for the non-equilibrium evaporation can be obtained in the following. Fig. 9 shows the variation of rupture time for the non-equilibrium as K varies. Let $\Im=0.1$, $\Re=1$, $\Omega=0$

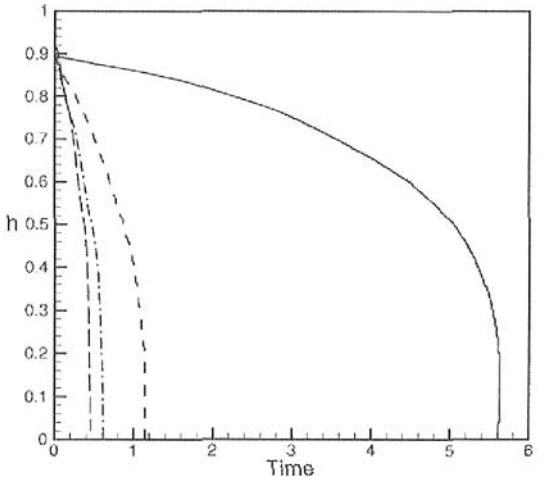

Fig. 7 The variation of rupture time for quasi-equilibrium evaporation as $\Im$ varies when $\Re=1$. Lines are for $\theta_r=0.389(\Im=1)$, $\theta_r=0.628$ $(\Im=0.6)$, $\theta=1.15(\Im=0.3)$ and $\theta_r=5.58(\Im=0)$ from the left. Initial value of liquid thickness (h) is 0.9

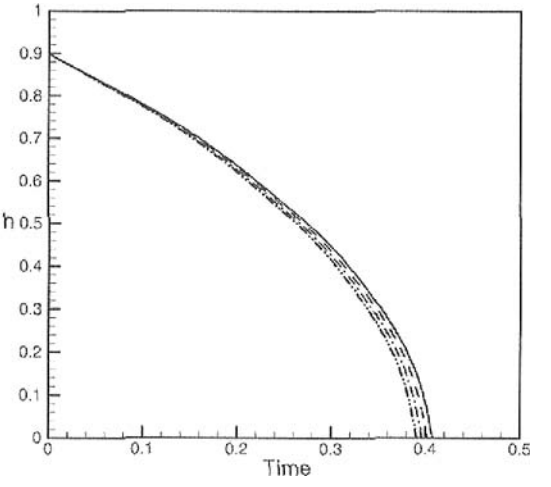

Fig. 8 The variation of rupture time for quasi-equilibrium evaporation as $\Re$ varies when $\Im=1$. Lines are $\theta_r=0.389(\Re=1)$, $\theta_r=0.40$ $(\Re=0.6)$, $\theta_r=0.4027(\Re=0.3)$ and $\theta_r=0.4082$ $(\Re=0)$ for from the left. Initial value of liquid thickness (h) is 0.9

for $K=0$, 0,3, 0.6, 0.9 1 and 10, respectively, make profiles for obtaining the film behavior, where

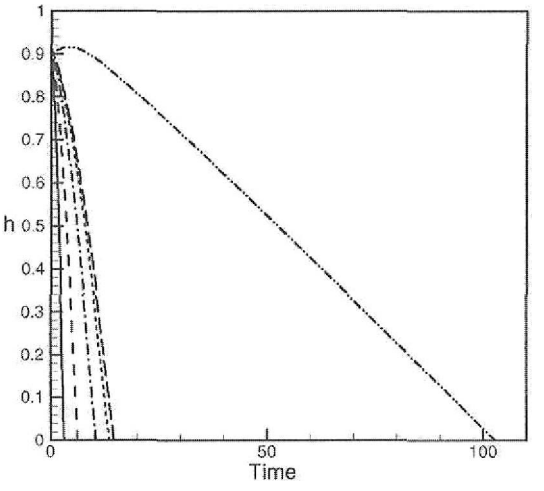

Fig. 9 The variation of rupture time for non quasi-equilibrium evaporation as K varies when $\Im=0.1$, $\Im=1$, $\Omega=0$. Lines are for $\theta_r=2.437$ $(K=0)$, $\theta_r=6.33(K=0.3)$, $\theta_r=9.37(K=0.6)$, $\theta_r=12.96(K=0.9)$, $\theta_r=14.02(K=1.0)$ and $\theta_r=104.98(K=10)$ from the left. Initial value of liquid thickness (h) is 0.9

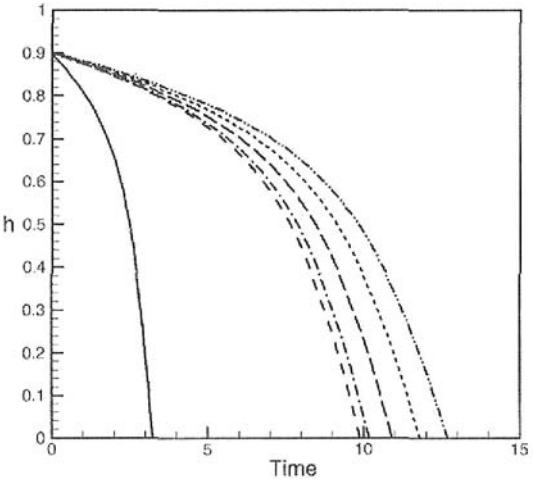

Fig. 10 The variation of rupture time for non quasi-equilibrium evaporation as Ω varies when $\Im=0$, $\Re=1$, $k=0.1$. Lines are for $\theta_r=3.69$ $(\Omega=10)$, $\theta_r=10.19(\Omega=0)$, $\theta_r=10.41(\Omega=0.9)$, $\theta_r=11.10(\Omega=0.6)$, $\theta_r=11.90(\Omega=0.3)$ and $\theta_r=12.836(\Omega=0)$ from the left. Initial value of liquid thickness (h) is 0.9

$\Omega=M\,\mathrm{Pr}^{-1}$ is the modified thermocapillarity. It is shown that the larger the value of K is, the longer rupture time is, and if $K\to\infty$ and $\theta_r\to\infty$, the result is produced like being isothermal.

Fig. 10 shows the variation of rupture time for the non-equilibrium as Ω varies. Let $\Im=0.1$, $\Re=1$, $K=0.1$, for $\Omega=0$, 0,3, 0.6, 0.9 1 and 10, respectively, make profiles for obtaining the film behavior. It is resulted that the larger the value of Ω is, the shorter rupture time is in the case of which the Non-equilibrium offset is small, moreover the vapor coil effect is considerable and the effect of the thermocapillarity is increasing. It can be expected how important the thermocapillarity

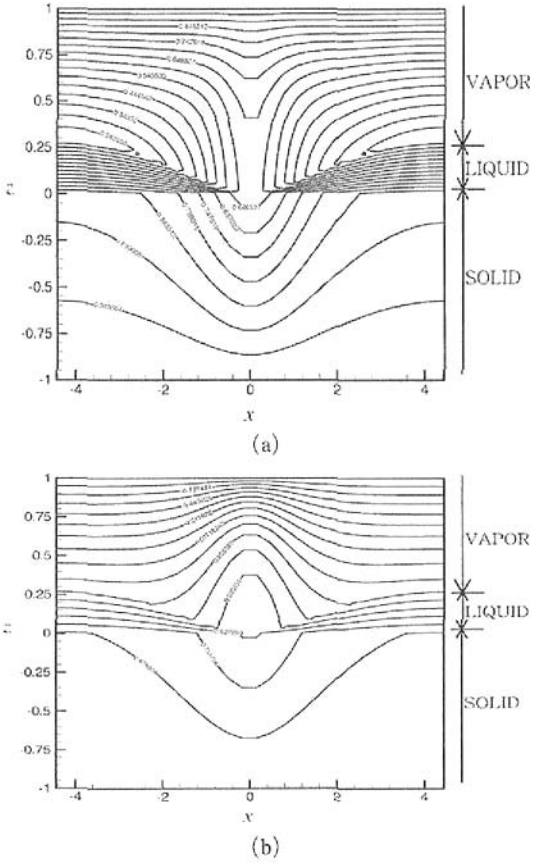

Fig. 11 Temperature of distribution at the rupture time when (a) $\Theta=1$ (at $z=1$) and (b) $\Theta=-1$ (at $z=1$) with $K\neq0$. Where the bottom of solid plate at $z=-1$, the top of solid plate is at $z=0$, and the water pipe is at $z=1$

is for rupture time.

4.4 Temperature distribution

Fig. 11 for the rupture time shows the temperature distribution when $\Theta=1$ and $\Theta=-1$ at $z=1$ with $K\neq 0$, respectively. In both of them each phases can be distinguished. The solid is at $z<0$, the liquid look like a hill with the crest at each sides and the trough at the center and the vapor is above the liquid. In the rupture time it can be observed that the rapid evaporation and its heat from the convection of vapor increases the temperature of vapor near the trough while the temperature of the solid plate locally decreases due to the heat loss to the trough shown in Fig. 11. it can make the unstable wave and different heat flux transferred.

5. Conclusions

We studied the behavior of the film liquid evaporation heated constantly under the solid plate, and we also analyzed in detail the basic state solution of the film behavior and the evolution equation expressing the film liquid motion containing the steep nonlinear characteristic with considering long wave disturbance in Eq. (101). The equation contains several physical factors such as the effect of vapor convection, mass loss, vapor recoil, thermocapillarity surface tension, and viscosity. Other authors (Burelbach, 1988; Panzarella, 2000) didn't show the effect of vapor convection in the system, and they were interested in only the behavior of the liquid-vapor interface.

They are important factors affecting to the expression of the behavior of the liquid film while the liquid film becomes thin evaporating at the liquid surface. Therefore, the interfacial temperature becomes unstable for the effect of the thermocapillary under the non-equilibrium evaporation. It results in the reduction of the mass loss rate and the reduction of the vapor recoil effect because of the increase of the liquid surface temperature heated from the solid plate as the film becomes thin. We also discussed the variation of solid, liquid and vapor temperature as the time becomes large. The convective effect in the vapor can be observed when $\Theta=1$ and $\Theta=-1$ at $z=1$. The temperature distribution around trough in case of $\Theta=1$ at $z=1$ is different from the case of $\Theta=-1$ at $z=1$. It can be also shown that the high temperature resulted from less evaporation, while the low temperature was from more evaporating to the vapor. These physical phenomena make the liquid film behavior unstable.

References

Bankoff, S. G., 1971, Intl. J. Heat Mass Transfer 14, pp. 377~385.

Burelbach, J. P., Bankoff, S. G. & Davis, S. H., 1988, 195, pp. 463~494.

Delhaye, J. M., 1974, Int. J. Multiphase Flow 1, pp. 395~409.

Davis, S. H. 1983, J. Applied Mech. Vol. 50, pp. 977~982.

Dussan, V. and Davis, S. H., 1974, J. Fluid Mech. 65, pp. 71~95.

Haley, J. P. and Miksis, M. J., 1991, J. Fluid Mech. Vol. 223, pp. 57~81.

Oron, A. and Davis, S. H. 1997, Rev. of Mod. Phys., Vol. 69, No. 3, pp. 931~979.

Panzarella, C. H., Davis, S. H. and Bankoff, S. G., 2000, J. Fluid Mech. Vol. 402, pp. 163~194.

Ruckenstenin, E. and Jain, R. K., 1974, J. Chem. Soc. Faraday Trans. II 70, pp. 132~147.

Vrij. A., 1966, "Possible Mechanism for the Spontaneous Rupture of Tin, Free Liquid Films." *Discuss. Faraday Sco.*, 42, pp. 23~33.

Williams, M. B. and Davis, S. H., 1982, J. Colloid Interface Sci., 90, pp. 220~228.

7. Appendix A

7.1

Dimensionless parameters in this paper

$$\mathrm{Pr}=\frac{\nu}{k}\quad G=\frac{D^3 g}{\nu}\quad D_\rho=\frac{\rho^v}{\rho}\quad D_v=\frac{\nu^v}{\nu}$$

$$\Gamma_s=\frac{\kappa^s}{\kappa}\quad \Gamma_v=\frac{\kappa^v}{\kappa}\quad R_s=\frac{k^s}{k}\quad R_v=\frac{k^v}{k}$$

$$E=\frac{k\Delta T}{\rho\nu L}\quad H=\frac{Dhr}{k}$$

$$K=\left(\frac{kT_{sat}^{3/2}}{aD\rho^{v}L^{2}}\right)\left(\frac{2\pi R_s}{M_w}\right)^{1/2}$$

$$D_\mu=\frac{\mu^v}{\mu}\quad L'=\frac{D^2L}{\nu^2}\quad S=\frac{\sigma_0 D}{\rho\nu^2}\quad C=\frac{\gamma\Delta T}{\sigma_0}$$

$$M=\frac{\gamma\Delta TD}{2\rho\nu\kappa}\quad \Theta=\frac{T_D-T_{sat}}{\Delta T}$$

7.2

The physical properties of liquid, WATER, are used in the simulation. Detailed data are listed in the following. A dimensionless parameter can be combined with them

$D=0.1\times10^{-5}$(m)	$\Delta T=10$(K)
$\rho=960$(kg/m^3)	$\rho^v=0.6$(kg/m^3)
$v=0.3\times10^{-6}$(m^2/s)	$v^v=0.21\times10^{-4}$(m^2/s)
$k=0.681$(W/mK)	$k^v=0.681$(W/mK)
$k^s=20(W/mK)$	$L=226\times10^4$(J/kg)
$\kappa=0.17\times10^{-6}$(m^2/s)	$\kappa^v=0.24\times10^{-4}$(m^2/s)
$M_w=10$(kg/kmol)	$R_s=8314$
$\sigma_0=0.0059$	$T_{sat}=373$(K)
$\gamma=0.18\times10^{-3}$	Pr$=1$
$D_\rho=1600$	$R_v=0.3\times10^{-3}$
$\Gamma_v=120$	$R_s=20$
$E=0.01$	$H=0.3\times10^{-4}$
$K=0.08$	$S=10$
$C=0.1$	$M=10$

7.3

Π, Π_1, Π_2, Π_3, Π_4 and Π_5 are

$$\Pi=\frac{\text{Pr}(D_\rho-1)R_B}{(R_B\Pi_2+d_b\Pi_1)\Gamma^v}$$

$$\Pi_1=HK+1$$

$$\Pi_2=HKh+K+h$$

$$\Pi_3=\Theta(R_B\Pi_2+d_b\Pi_1)-R_BK$$

$$\Pi_4=R_s(K+h)+d_b$$

$$\Pi_5=2D_\rho R_s^3E^2$$